ECCOMAS Congress 2016
VII European Congress on Computational Methods in Applied Sciences and Engineering
M. Papadrakakis, V. Papadopoulos, G. Stefanou, V. Plevris (eds.)
Crete Island, Greece, 5–10 June 2016

A CONTINUOUS ADJOINT APPROACH FOR VEHICLE INTERIOR NOISE REDUCTION

Christos Kapellos[1] **and Michael Hartmann**[1]

[1]Volkswagen AG, Group Research, CAE Methods
Letter Box 1777, D-38436, Wolfsburg, Germany
e-mail: {christos.kapellos,michael.hartmann2}@volkswagen.de

Keywords: continuous adjoint method, vibroacoustics, automotive noise reduction

Abstract. *In this paper the continuous adjoint method is developed for a vibroacoustic model that predicts the interior noise of a vehicle induced by the airflow. The model simulates the front side window vibration, excited by the acoustic and hydrodynamic pressure load, and the resulting sound wave propagation into the cabin. Targeting interior noise reduction, the continuous adjoint formulation is used to derive the adjoint to the state equations, namely the bending wave and the wave equations, whilst taking into consideration their coupling. The developed method is applied to a generic vehicle test body for the minimisation of the interior noise.*

1 INTRODUCTION

When a vehicle travels at high speeds wind noise dominates the noise perceived in the passenger cabin. The turbulent flow field around the A-pillar and side mirror induce flunctuating acoustic and hydrodynamic pressure load on the side window. The vibrational response in form of bending waves of the window generates in turn sound waves which propagate to the interior and contribute to the overall sound pressure level.

In [1], the external flow generated sound and its propagation into the interior of a model passenger vehicle was numerically and experimentally investigated. The vehicle model, which is also used in this paper, was a SAE Type 4 car body and was built in such a way that only sound transmission through the front side and only window is allowed. In [2] a vibroacoustic model was developed to simulate the window vibration induced by pressure load and afterwards the sound propagation in the interior of the same vehicle.

In this paper the continuous adjoint method is developed for the aforementioned vibroacoustic model, in order to compute gradients of functionals related to the interior noise of a vehicle. Continuous and discrete adjoint methods [3, 4] have been widely used to solve optimisation problems in various research fields, due to their advantage of computing cost function gradients at a computational cost nearly independent of the number of the design variables. In the continuous formulation, the adjoint equations and sensitivity derivatives are derived by differentiating the objective function, augmented by the field and time integral of the product of the state equations and the adjoint variables. The adjoint equations are discretised and numerically solved to compute the adjoint fields and, through them, the sensitivity derivaties. In contrast, the discrete adjoint equations are derived directly from the discretised state equations. This paper is dealing exclusively with the continuous adjoint method.

2 VIBROACOUSTIC MODEL FOR THE INTERIOR NOISE OF A VEHICLE

The governing equation of the window deflection driven by a given pressure load is the two-dimensional bending wave equation,

$$R^w = \frac{\partial^2 w}{\partial t^2} + \frac{D}{m'}\nabla^4 w + \eta_1 \frac{D}{m'}\frac{\partial}{\partial t}\nabla^4 w + \eta_2 \frac{\partial w}{\partial t} + \eta_3 \sqrt{\frac{D}{m'}}\frac{\partial}{\partial t}\nabla^2 w - \frac{p'}{m'} = 0 \tag{1}$$

where w is the window deflection, p' the pressure load, D the window bending stiffness, m' the normalised window mass and η_i the damping coefficients. The initial and boundary conditions for a pinned at its edges window are

$$w = 0 \quad \text{and} \quad \frac{\partial w}{\partial t} = 0 \ \text{ for } t = 0s \text{ and } \mathbf{x} \in S_{wi} \tag{2}$$

$$w = 0 \quad \text{and} \quad \nabla^2 w = 0 \ \text{ for } \mathbf{x} \in \partial S_{wi} \text{ and } t > 0s \tag{3}$$

where S_{wi} is the window surface.

The window vibration generates sound waves which propagate to the vehicle interior. The sound radiation is governed by the wave equation,

$$R^p = \frac{\partial^2 p}{\partial t^2} - c^2 \nabla^2 p = 0 \tag{4}$$

The initial and boundary conditions are

$$p = 0 \text{ and } \frac{\partial p}{\partial t} = 0 \quad \text{for} \quad t = 0s \text{ and } \mathbf{x} \in \Omega \tag{5}$$

$$\nabla p \cdot \mathbf{n} = \rho_0 \frac{\partial^2 w}{\partial t^2} \quad \text{for} \quad \mathbf{x} \in S_{wi} \subset \partial\Omega \text{ and } t > 0s \tag{6}$$

$$\nabla p \cdot \mathbf{n} = -\frac{1}{c}\frac{\partial p}{\partial t} \quad \text{for} \quad \mathbf{x} \in S_{wa} \subset \partial\Omega \text{ and } t > 0s \tag{7}$$

where Ω is the interior domain and $\partial\Omega = S_{wi} \cup S_{wa}$. On the window S_{wi}, the acoustic pressure is coupled with the window accelaration. At any other interior wall the propagated sound waves are reflected and a convective boundary condition is imposed.

The equations are programmed and solved in OpenFOAM, version 1.6-ext. For the solution of the bending wave equation a fourth order scheme for gradients, a first order scheme for second order time derivatives and an explicit time marching scheme were used. Moreover, in order to take into account the difference of propagation speeds of waves in the window and in the air, the bending wave equation is solved with a smaller timestep.

3 THE CONTINUOUS ADJOINT FORMULATION FOR THE VIBROACOUSTIC MODEL

The objective function to be minimised is defined as the integral over a time interval T of the squared pressure at a specific point P

$$J = \frac{1}{T}\int_T p_P^2 \, dt \tag{8}$$

The implentation of more sophisticated objective functions, such as functionals in frequency domain, is possible. However, without loss of generality, a simplified objective function was chosen here so as to clearly focus on the results of the developed method.

The augmented function L is defined as the sum of J and the time-space integrals of the product of the state equations and the corresponding adjoint variables. So,

$$L = J + \int_T \int_{S_{wi}} z R^w dS dt + \int_T \int_\Omega q R^p dV dt \tag{9}$$

where z and q are the adjoint deflection and pressure respectively. Next step is to compute the variation of L

$$\delta L = \delta J + \int_T \int_{S_{wi}} z \delta R^w dS dt + \int_T \int_\Omega q \delta R^p dV dt \tag{10}$$

The development using the Gauss divergence theorem of steady and unsteady terms similar to the ones of eq. 10 has been thoroughly covered in literature [5], and is therefore omitted here. Due to the self-adjoint nature of the state equations, the adjoint equations will have the same differential operators, now applied on the adjoint variables, apart from the first order derivatives, which will appear with the opposite sign in the adjoint equations.

More focus is laid upon the the derivation of the boundary conditions and sensitivity derivatives on the window and how the coupling between the two adjoint equations is achieved. The surface integrals expressed on the window derived by the expansion of $\int_T \int_\Omega q \delta R^p dV dt$ read

$$c^2 \int_T \int_{S_{wi}} \left[\nabla q \cdot \mathbf{n} \, \delta p - q \, \delta \left(\nabla p \cdot \mathbf{n} \right) \right] dS dt \tag{11}$$

The first term is set to zero, by imposing a zero Neumann boundary condition for adjoint pressure q on the window. Using eq. 6 , the second term expands further to

$$\rho_0\, c^2 \int_T \int_{S_{wi}} -q \left(\frac{\partial^2 \delta w}{\partial t^2} \right) dS dt = \rho_0\, c^2 \int_{S_{wi}} \left[-q \frac{\partial \delta w}{\partial t} + \frac{\partial q}{\partial t} \delta w \right]_{T_{start}}^{T_{end}} dS + \rho_0\, c^2 \int_T \int_{S_{wi}} -\frac{\partial^2 q}{\partial t^2} \delta w \, dS dt \tag{12}$$

All terms of eq. 12 include now the total variation of the deflection w. The first integral gives the initial conditions for the adjoint wave equation, while the second one will be the source term for the adjoint bending wave equation.

The **adjoint equations** and their respective **boundary conditions** eventually read

$$R^q = \frac{\partial^2 q}{\partial t^2} - c^2 \nabla^2 q + 2 p_P = 0 \tag{13}$$

with

$$q = 0 \text{ and } \frac{\partial q}{\partial t} = 0 \quad \text{for} \quad t = T_{end} \text{ and } \mathbf{x} \in \Omega \tag{14}$$

$$\nabla q \cdot \mathbf{n} = \frac{1}{c} \frac{\partial q}{\partial t} \quad \text{for} \quad \mathbf{x} \in S_{wa} \subset \partial\Omega \text{ and } t < T_{end} \tag{15}$$

$$\nabla q \cdot \mathbf{n} = 0 \quad \text{for} \quad \mathbf{x} \in S_{wi} \subset \partial\Omega \text{ and } t < T_{end} \tag{16}$$

and

$$R^z = \frac{\partial^2 z}{\partial t^2} + \frac{D}{m'} \nabla^4 z - \eta_1 \frac{D}{m'} \frac{\partial}{\partial t} \nabla^4 z - \eta_2 \frac{\partial z}{\partial t} - \eta_3 \sqrt{\frac{D}{m'}} \frac{\partial}{\partial t} \nabla^2 z - c^2 \rho \frac{\partial^2 q}{\partial t^2} = 0 \tag{17}$$

with

$$z = 0 \quad \text{and} \quad \frac{\partial z}{\partial t} = 0 \text{ for } t = T_{end} \text{ and } \mathbf{x} \in S_{wi} \tag{18}$$

$$z = 0 \quad \text{and} \quad \nabla^2 z = 0 \text{ for } \mathbf{x} \in \partial S_{wi} \text{ and } t < T_{end} \tag{19}$$

The **sensitivity derivatives** expression of the objective function with respect to any design variables b_m which affect the input pressure load is given by

$$\frac{\delta J}{\delta b_m} = - \int_T \int_{S_{wi}} \frac{z}{m'} \frac{\delta p'}{\delta b_m} dS dt \tag{20}$$

In the adjoint chain, the procedure is performed backwards in time and in reverse order. The variation of the objective function acts as a monopole source for the adjoint wave equation and the information propagates to the interior. Then, the second derivative of the adjoint pressure on the window is used as a source term for the adjoint bending wave equation. In the end, the sensitivity derivatives computed at the window express the change in the objective function induced by a change in pressure load p'.

In case there is a closed-form expression for p', as in the test case shown in section 5, the gradient of the pressure load can be analytically calculated. Otherwise, when p' is derived from the solution of another set of equations, the right hand side term in eq. 20 serves as a boundary condition to its corresponding adjoint. For example, in case p' is the hydrodynamic pressure computed by solving the incompressible Navier-Stokes equations, the integrad of 20 is used for imposing the boundary condition for the adjoint Navier-Stokes on the window.

4 VALIDATION OF THE METHOD

The accuracy of the adjoint solution was validated first for each equation separately and then for the coupled problem, thus for three different cases. The vehicle model used is the SAE Body, seen in fig. 1.

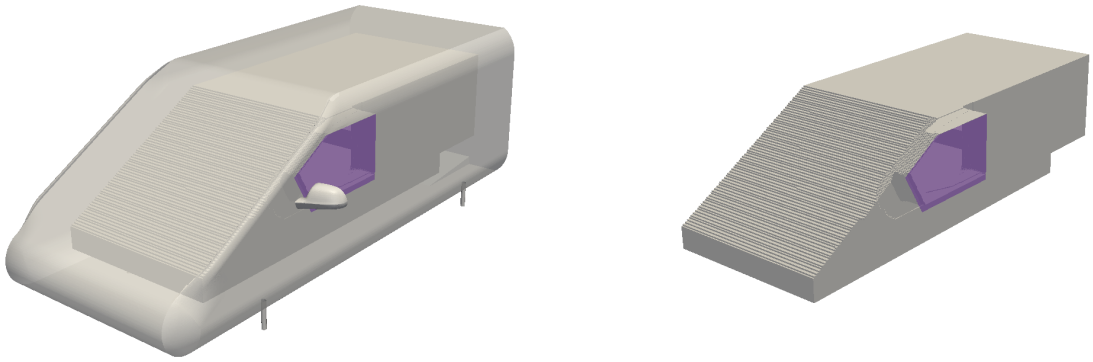

Figure 1: SAE Type 4 geometry: Exterior (left) and interior (right) vehicle walls. The only window of the vehicle, through which sound is transmitted to the interior, is coloured in magenta.

For the window vibration a plane wave excitation is investigated, targeting at minimising the time averaged square of the deflection,

$$p'_{vib} = A\sin(k_x x - \omega t) \text{ and } J_{vib} = \frac{1}{T}\int_T \int_{S_{wi}} w^2 dSdt \tag{21}$$

For sound radiation in the interior a plane wave profile is given for w in eq. 6 , targeting at minimising the objective function in 8.

$$w_{prop} = A\sin(k_x x - \omega t) \text{ and } J_{prop} = \frac{1}{T}\int_T \int_{S_{wi}} p_P^2 dSdt \tag{22}$$

For the coupled problem the plane wave excitation of eq. 21 was used.

$$p'_{coupl} = A\sin(k_x x - \omega t) \text{ and } J_{coupl} = \frac{1}{T}\int_T \int_{S_{wi}} p_P^2 dSdt \tag{23}$$

The gradient of the respective objective function for each of the three aforementioned testcases with respect to the input amplitude were computed with the continuous adjoint method and compared with finite differences.

As seen in table 1, the continuous adjoint method computes the gradient of the objective function with sufficient accuracy, since at most occasions the relative error is lower than 1%. In the sound radiation case, the higher error can be explained by taking into consideration the boundary condition on the window. Since the given deflection w_{prop} does not fulfil a zero Dirichlet condition on the window edges, a discontinuity arises there, which leads to higher numerical errors. However, the high accuracy computation in the coupled problem means that the gradient can be confidently used in a gradient-based optimisation.

	Window Vibration	Sound propagation	Coupled Problem
Continuous Adjoint	2.4391E-15	6.236	3.115E-10
Finite Differences	2.4394E-15	6.486	3.085E-10
Relative Error (%)	0.013	3.87	-0.964

Table 1: Comparison between objective function gradient values computed with the continuous adjoint method and finite differences.

5 MINIMISING THE INTERIOR NOISE OF THE SAE BODY

The developed method was applied for the minimisation of the perceived noise near the driver's ear, in the SAE body. To keep a focus only on the vibroacoustic phenomena and their adjoint, the pressure load on the window was induced by the sound radiation from a dipole source in a moving medium, rather than by a fully developed turbulent flow. The induced pressure is given analytically by

$$p'(\mathbf{x},t) = -\rho_0 \left[\frac{\partial}{\partial t} + U_0 \nabla\right] \phi \tag{24}$$

where ρ_0 is the air density, U_0 the vehicle velocity and ϕ the acoustic potential

$$\phi(\mathbf{x},t) = \nabla \left\{ \frac{A}{4\pi R^*} e^{i\omega\left(t-\frac{R^+}{c_0}\right)} \right\} \mathbf{d} \tag{25}$$

with amplitude A and directivity vector $\mathbf{d}$. Variables R^+ and R^* are related to the distance between the dipole and each receiver point where the induced pressure is calculated [6], namely each computational face of the window, S_{wi}.

Optimising with respect to its position, the dipole source is only allowed to move on the surface of an ellipsoid resembling a vehicle mirror, as seen in fig. 3. Moreover, its directivity is defined by the normal to the surface vector. The design variables of the optimisation problem are variables u and v which parameterise the ellipsoid surface by

$$\begin{aligned} X_{dip} &= X_c + a\cos u \cos v \\ Y_{dip} &= Y_c + b\cos u \sin v \\ Z_{dip} &= Z_c + c\sin u \end{aligned} \tag{26}$$

with $-\frac{\pi}{2} \leq u \leq \frac{\pi}{2}$ and $-\pi \leq v \leq \pi$

By differentiating eqs. 24 ,25 and 26, a closed form expression is derived for the derivative of the pressure load with respect to the design variables in expression 20.

A linesearch strategy was used for updating the design variables, starting from the initial value $\mathbf{b}^{init} = (0\ 0)$. The quasi-Newton BFGS method was used for computing the search direction and an interpolation based algorithm for choosing an appropriate step length [7]. In total 4 optimisation cycles were performed and the objective function was reduced by 34.3%. As seen in fig. 4, the dipole source is moved by the optimisation algorithm in a way that the induced pressure amplitude is reduced and that less area is affected by the dipole source. The first is achieved by increasing the distance between the source and the window and the second by pointing the directivity parallel to the z-axis.

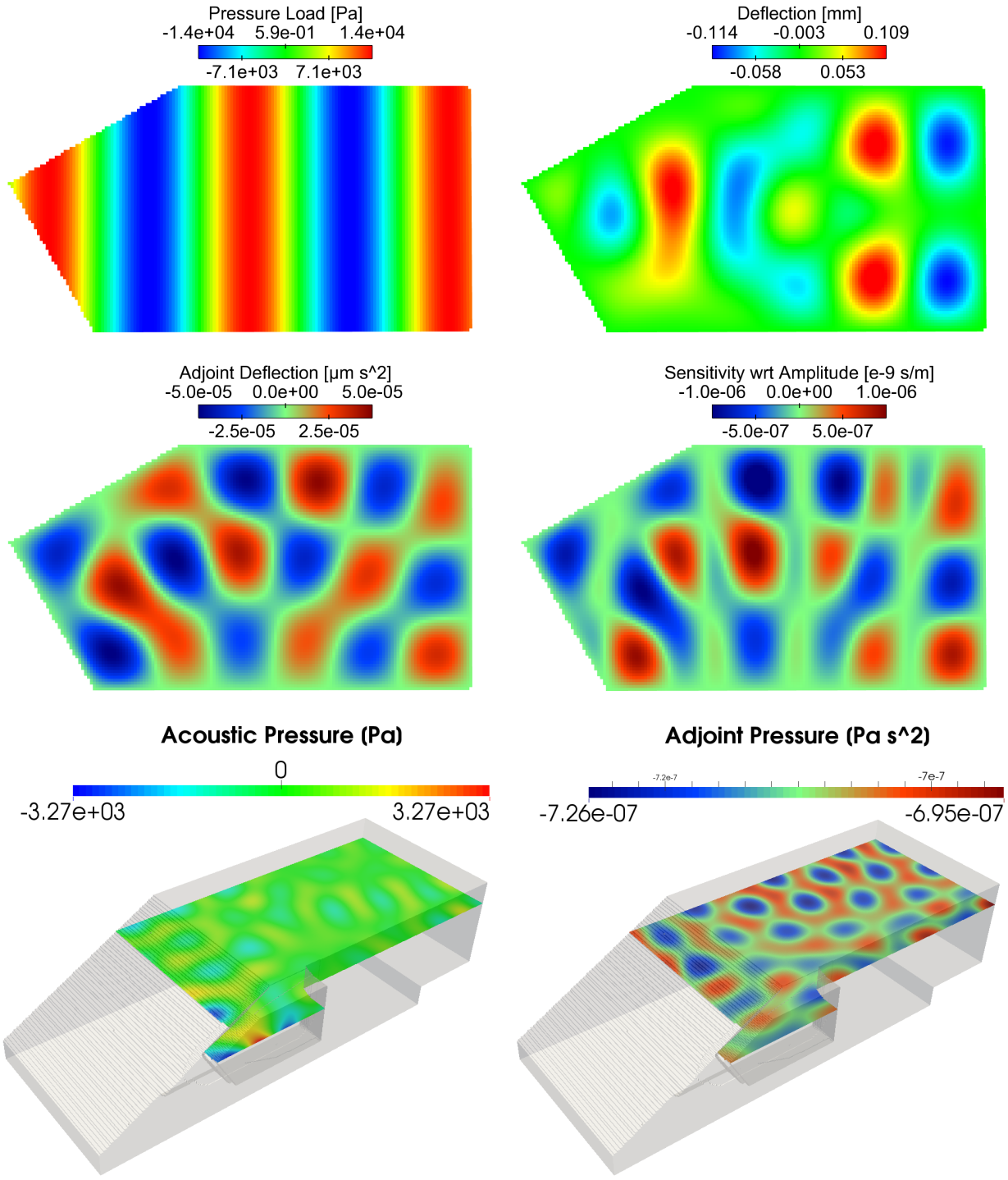

Figure 2: Validation of the adjoint solution. Bending wave equation: Instantaneous fields of the input pressure load p'_{vib} (top left), window deflection w (top right), adjoint deflection z (middle left) and sensitivity derivative w.r.t. input amplitude (middle right). Wave equation: Instantaneous fields of pressure (bottom left) and adjoint pressure (bottom right).

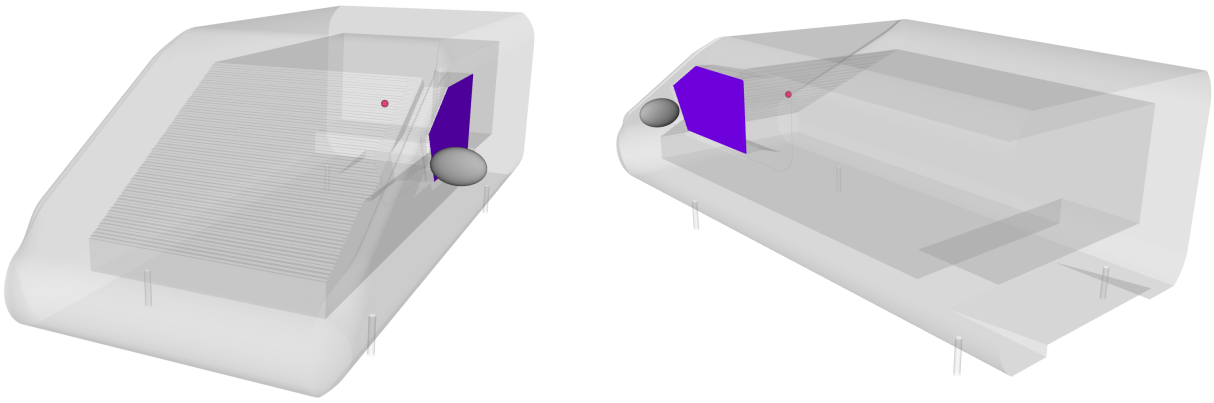

Figure 3: Minimising the interior noise of the SAE body: Pressure load on the window is induced by a dipole source which moves on the surface of the ellipsoid resembling a mirror, with directivity normal to the surface. The optimisation loop will find the optimal position of the dipole source, so that the perceived noise at the point near the driver's ear (red sphere) is reduced.

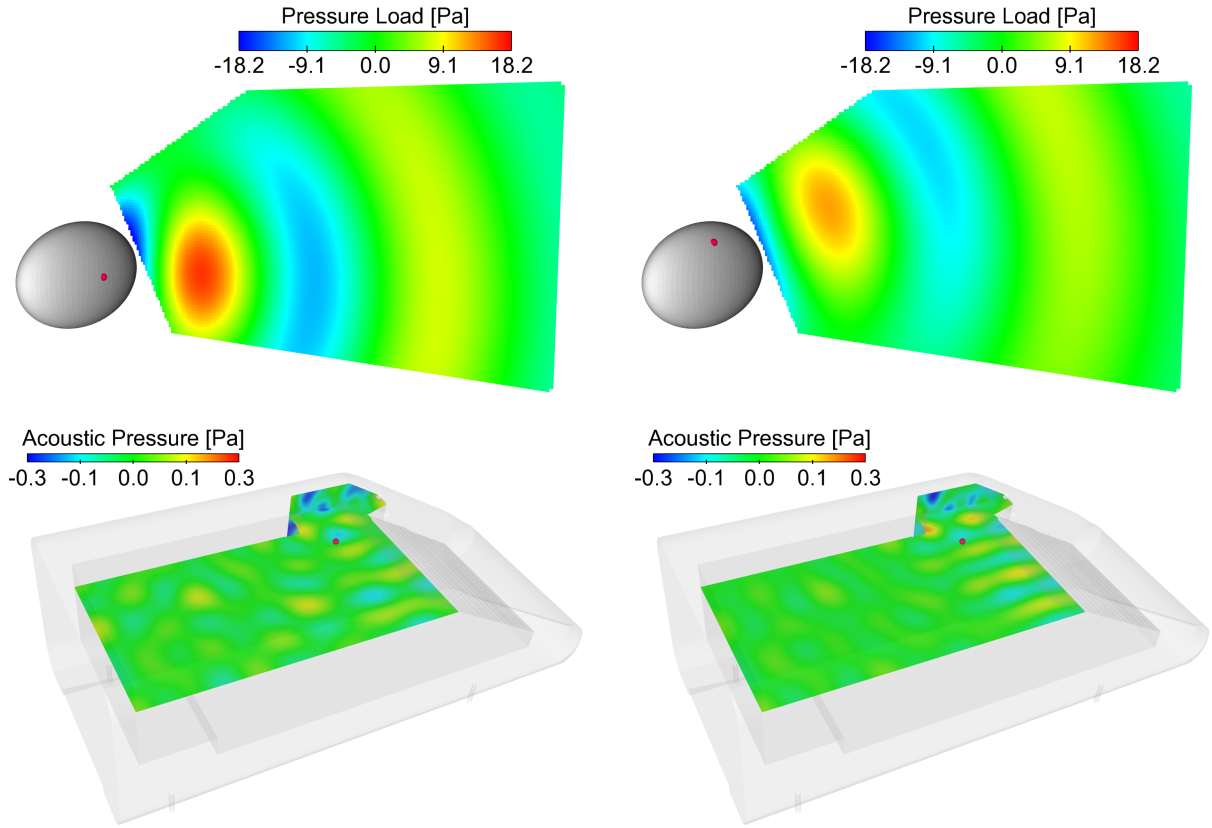

Figure 4: Minimising the interior noise of the SAE body: Comparison between the starting (left) and the optimised (right) setup. The instantaneous pressure load p' (top row) induced by the dipole source (red sphere) has reduced amplitude and acts on a smaller area of the window in the optimised case. The amplitude of the acoustic pressure in the interior computed at a time instance (bottom row) is also reduced for the optimal position of the source.

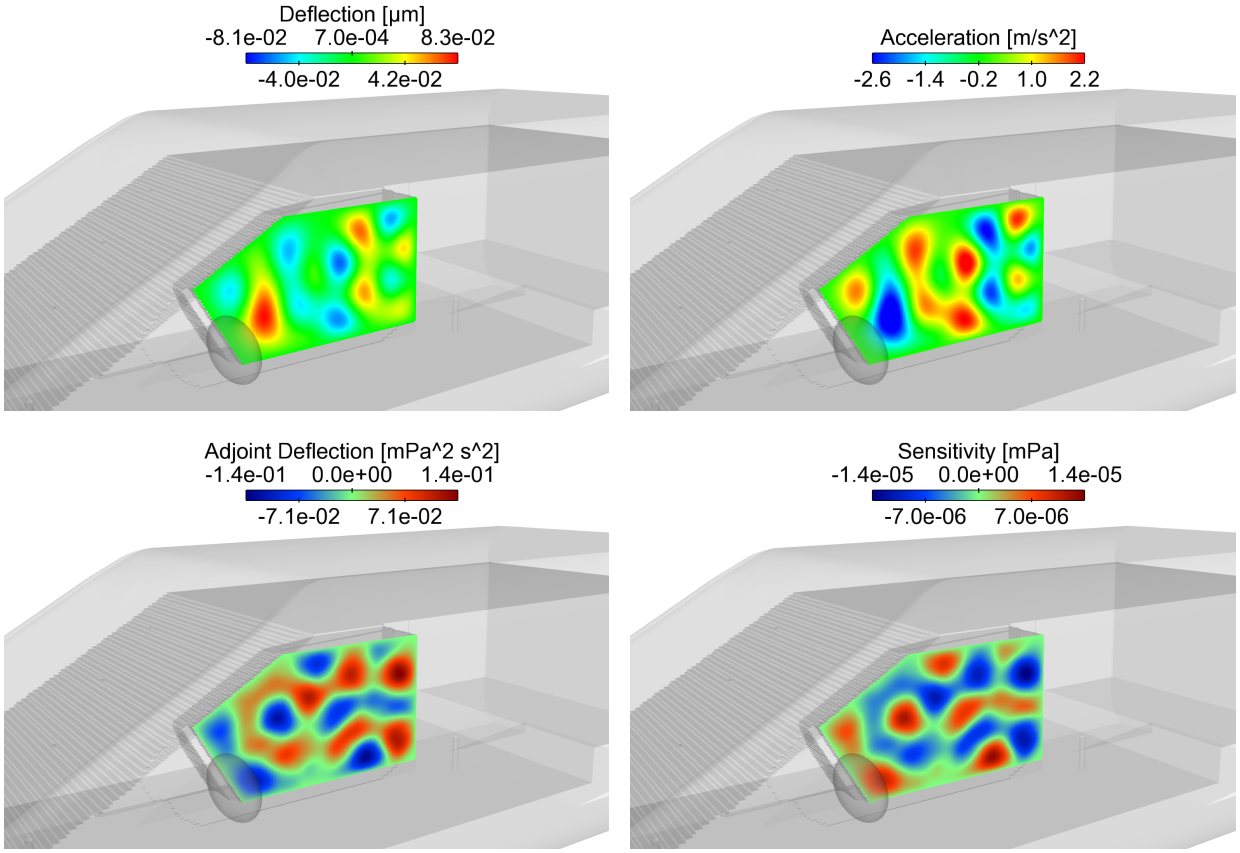

Figure 5: Minimising the interior noise of the SAE body: Instantaneous fields of deflection (top left) and acceleration (top right) of the window, as well as adjoint deflection (bottom left) and sensitivity (bottom right) computed at the first optimisation cycle.

6 CONCLUSIONS

The continuous adjoint method was formulated for a vibroacoustic model, which predicts the vehicle interior noise induced by a pressure load on the side window. The primal equations include the bending wave equation, which simulates the vibrational response of the window to the pressure load, and the wave equation, which describes the sound radiation to the interior. The adjoint to the state equations and the corresponding boundary conditions which couple the two equations were derived.

The method was validated with finite differences and applied to interior noise reduction in a generic vehicle model, the SAE body. In this case, the pressure load was induced by the sound radiation from a dipole source located at the area of the side mirror and the optimisation algorithm searched for the optimal position of the source. It was shown that the developed method computes gradients with sufficient accuracy and therefore can be integrated to larger aeroacoustic chains, in which the pressure load on the window is computed by solving different sets of equations, such as the Navier-Stokes equations.

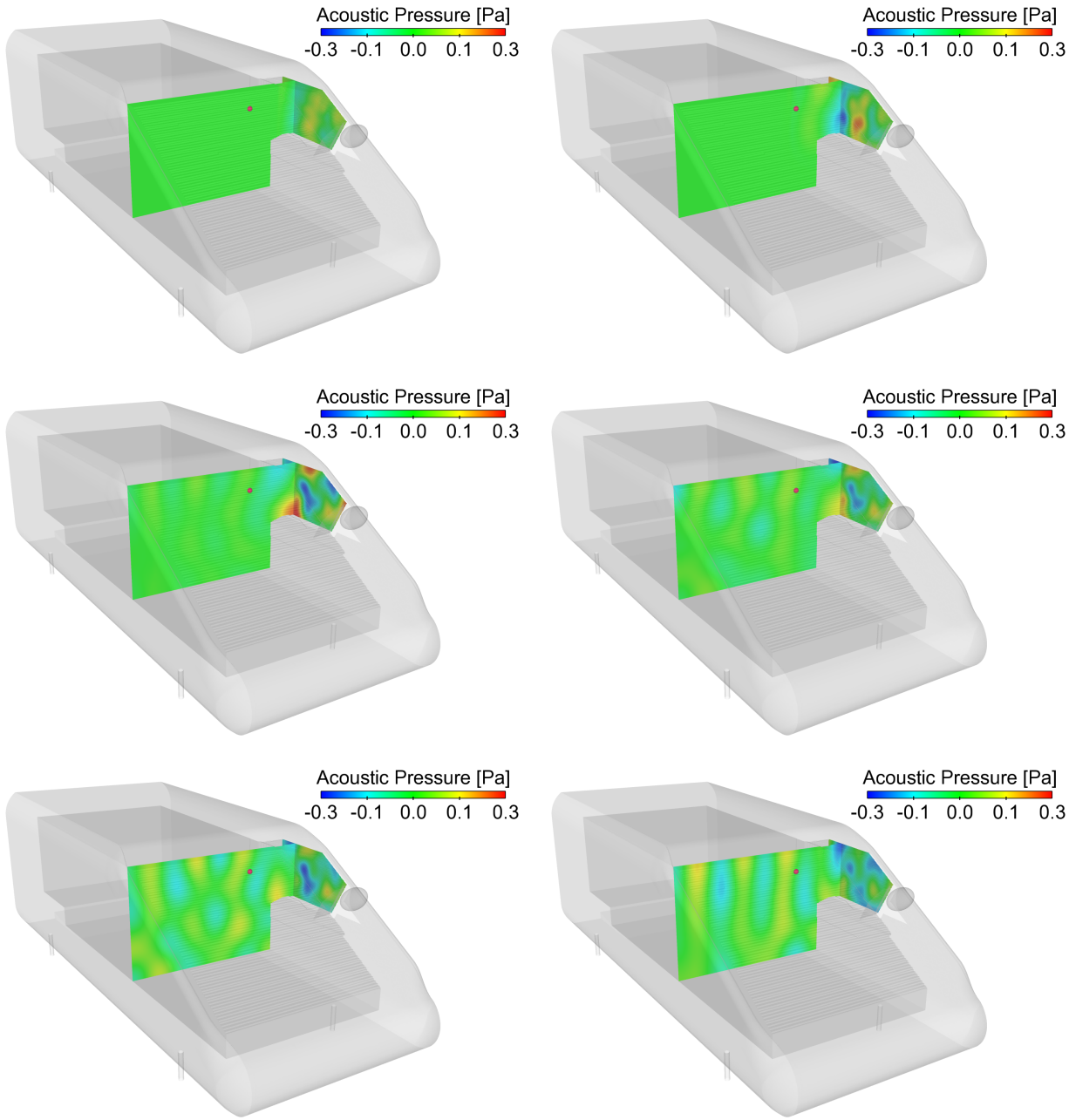

Figure 6: Minimising the interior noise of the SAE body: Six time snapshots during the sound radiation in the interior, computed at the first optimisation cycle. Sound waves generated by the window vibration propagate to the interior and are partly reflected by the vehicle interior walls.

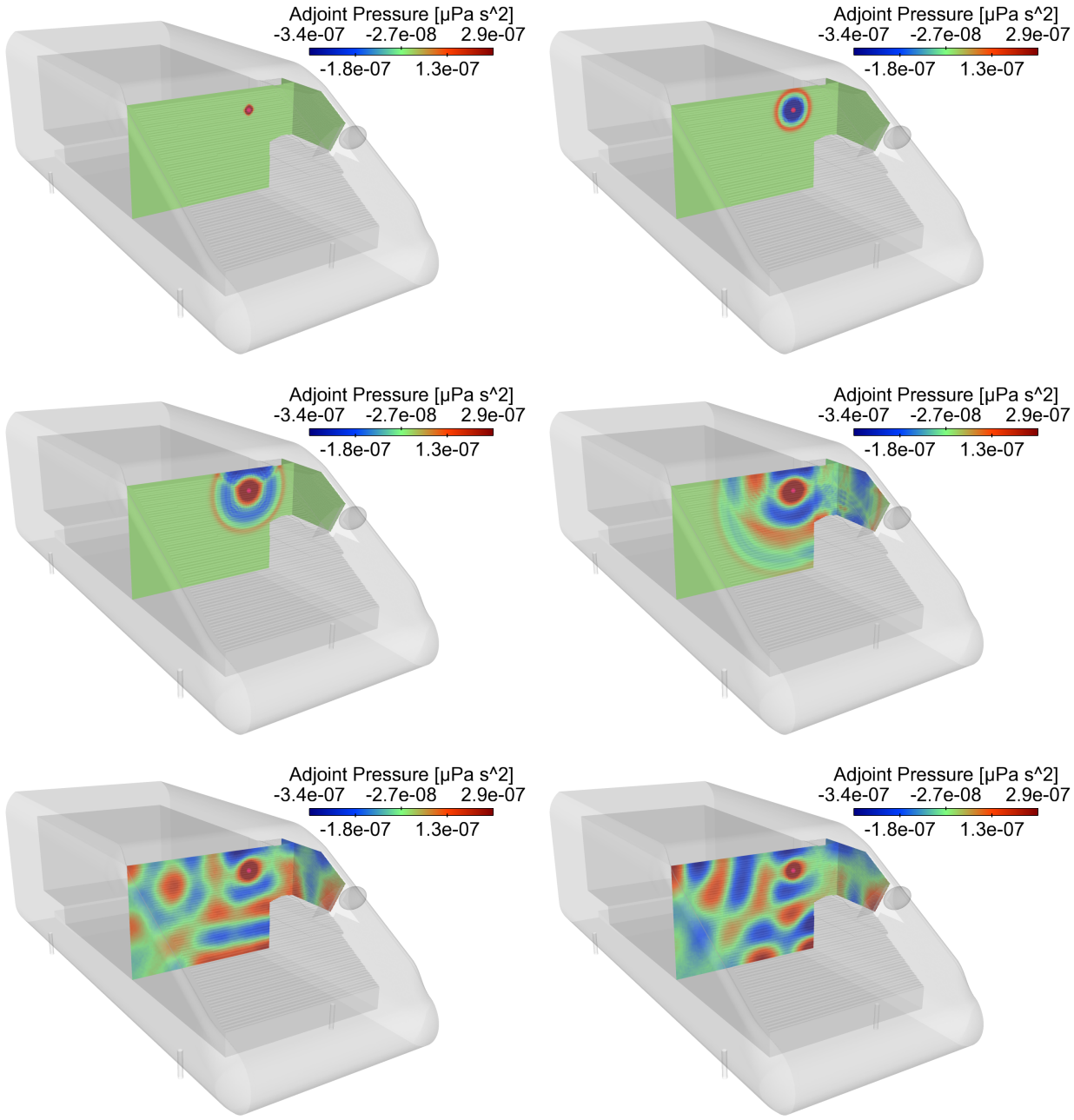

Figure 7: Minimising the interior noise of the SAE body: Six time snapshots of the computed adjoint pressure. The point where the objective function is defined (red sphere) acts as a monopole source for the adjoint wave equation. The adjoint pressure flunctuations propagate to the interior and reach the window. The second time derivative of the presented field at the window is the source for the adjoint bending wave equation.

REFERENCES

[1] M. Hartmann, J. Ocker, T. Lemke, A. Mutzke, C. Schwarz, H. Tokuno, R. Toppinga, P. Unterlechner, G. Wickern, Wind Noise caused by the A-pillar and the Side Mirror flow of a Generic Vehicle Model. *18^{th} AIAA/CEAS Aeroacoustics Conference (33^{rd} AIAA Aeroacoustics Conference)*, 2012, Colorado Springs, USA

[2] Alexander Kabat vel Job, Analysis of the vibrational response of a non-laminated glass plate for predicting the aeroacoustic performance in time domain. *The 2^{nd} OpenFOAM User Conference 2014*, Berlin Germany

[3] S. Nadarajah, A. Jameson, Studies of the continuous and discrete adjoint approaches to viscous automatic aerodynamic shape optimisation. *AIAA Paper*, 25(30), 2001

[4] M. Giles, N. Pierce, An introduction to the adjoint approach to design. *Flow, Turbulence and Combustion*, 65,393-415, 2000

[5] E. Papoutsis-Kiachagias, K. Giannakoglou, Continuous adjoint methods for turbulent flows, applied to shape and topology optimization: Industrial applications. *Archives of Computational Methods in Engineering*, 2014, 1-45

[6] A. Najafi-Yazdi, F. Bres, L. Mongeau, An acoustic analogy formulation for moving sources in uniformly moving media. *Proceedings of the Royal Society A*, 2010

[7] J. Nocedal, S. Wright, Numerical Optimization. *Springer*